REPORT DOCUMENTATION PAGE

Form Approved
OMB NO. 0704-0188

1. AGENCY USE ONLY (Leave Blank)	2. REPORT DATE December 15, 1999	3. REPORT TYPE AND DATES COVERED FINAL

4. TITLE AND SUBTITLE
Study of Ice Adhesion with SFM and Electro-Magnetic Measurements

5. FUNDING NUMBERS
DAAH-04-95-1-0189

6. AUTHOR(S)
Victor F. Petrenko

7. PERFORMING ORGANIZATION NAME(S) AND ADDRESS(ES)
Thayer School of Engineering, Dartmouth College
HB 8000 Hanover NH 03755

8. PERFORMING ORGANIZATION REPORT NUMBER

9. SPONSORING / MONITORING AGENCY NAME(S) AND ADDRESS(ES)
U. S. Army Research Office
P.O. Box 12211
Research Triangle Park, NC 27709-2211

10. SPONSORING / MONITORING AGENCY REPORT NUMBER
ARO 34527.2-EV

11. SUPPLEMENTARY NOTES
The views, opinions and/or findings contained in this report are those of the author(s) and should not be construed as an official Department of the Army position, policy or decision, unless so designated by other documentation.

12 a. DISTRIBUTION / AVAILABILITY STATEMENT
Approved for public release; distribution unlimited.

12 b. DISTRIBUTION CODE

13. ABSTRACT (Maximum 200 words)

The goal of this project was to gain a basic knowledge on ice adhesion.
In the course of the research we have studied experimentally and theoretically two of three main physical mechanisms of ice adhesion: electrostatic interactions and hydrogen bonding. The contribution of the last mechanism, van der Waals interaction, was determined as a difference between the total adhesion and the former two mechanisms. Two new physical phenomena were discovered: the effect of DC potential on adhesion of ice to metals and effect of ice electrolysis on ice adhesion. One book (Physics of Ice) and 8 papers were published and one patent was issued on the results of the project. Three invited talks (one in Japan) and six conference presentation were given. The grant supported two graduate and two undergraduate students at Dartmouth College.

14. SUBJECT TERMS
Ice, Ice Adhesion, Scanning Force Microscopy, Ice Surface

15. NUMBER OF PAGES

16. PRICE CODE

17. SECURITY CLASSIFICATION OR REPORT	18. SECURITY CLASSIFICATION ON THIS PAGE	19. SECURITY CLASSIFICATION OF ABSTRACT	20. LIMITATION OF ABSTRACT
UNCLASSIFIED	UNCLASSIFIED	UNCLASSIFIED	UL

REPORT DOCUMENTATION PAGE (SF298)
(Continuation Sheet)

List of manuscripts:

Journal Publications:

1. N. N. Khusnatdinov and V. F. Petrenko: Experimental study of ice electrolysis in darkness and under ultraviolet irradiation. Journal of Physical Chemistry, vol. 101, 6208-6211 (1997).
2. N. N. Khusnatdinov, V. F. Petrenko, and C. Levey: Electric properties of ice/solid interface. Journal of Physical Chemistry, vol. 101, 6212-6214 (1997).
3. V. F. Petrenko: Study of ice surface and ice/solid interfaces with scanning force microscopy. Journal of Physical Chemistry, vol. 101, 6276-6281 (1997).
4. I. A. Ryzhkin and V. F. Petrenko: Physical mechanisms responsible for ice adhesion. Journal of Physical Chemistry, vol. 101, 6267-6270 (1997).
5. V. F. Petrenko and I. A. Ryzhkin: Surface states of charge carriers and electric properties of the surface layer of ice. Journal of Physical Chemistry, vol. 101, 6285-6289 (1997).
6. V. F. Petrenko: Effect of electric fields on ice adhesion to mercury. Journal of Applied Physics, vol. 84, 261-267 (1998).
7. V. F. Petrenko and S. Qi: Effect of electric field on ice adhesion to stainless steel. Journal of Applied Physics, vol. 86, 5450-5454 (1999).

Other Publications:

8. V. F. Petrenko: Methods and apparatus for modifying ice adhesion strength. World Intellectual Property Organization. PCT. International Publication Number WO 98/57851, 23 December 1998.

Book:

9. V. F. Petrenko and R. W. Whitworth: Physics of Ice. Oxford University Press (1999).

Sientific personnel supported:

1. Victor F. Petrenko, PI, Research Professor of Engineering.
2. Douglas Trickett, PhD student
3. Zoe Courville, PhD student
4. Rafael Hernandez, undergraduate (work-study) student
5. Frank Black, undergraduate student

Report of Inventions

1. Systems and Method for modifying Ice Adhesion Strength. United States Patent #6,027,075, Feb 22, 20000.
2. USP Provisional Application, Attorney docket No. 4503/009P, filed October 27, 1998.
3. USP Provisional Application, Attorney docket No. 4503/009P2, filed December 1, 1998.
4. USP Provisional Application, Attorney docket No. 4503/009P3, filed March 1, 1999.
5. USP Provisional Application, Attorney docket No. 4503/009P4, filed April 23, 1999.
6. World Intellectual Property Organization (WIPO) patent application, WO9857851A2, filed December 23, 1998.

Scientific progress and accomplishments:

SEE ATTACHMENT I

STUDY OF ICE ADHESION WITH SFM AND ELECTROMAGNETIC MEASUREMENTS

FINAL REPORT
GRANT # DAAH-04-95-1-0189

PI: Victor F. Petrenko
Thayer School of Engineering, Dartmouth College, Hanover, NH 03755

List of Content

Problem definition

Icing of airplanes, helicopters, ships and power lines, and icy roads are costly and dangerous problems. The development of coatings with very low adhesion to ice would solve these problems once and for all. However, ice strongly adheres to a wide variety of solids, even to hydrophobic material. A good solution requires a fundamental understanding of the physical mechanisms of bonding between ice and other solids. Ice adhesion is a complex problem, and the trial and error approaches used so far, that is, testing candidate materials to see if they exhibit low adhesion, are unlikely to lead to a solution. A good solution requires a fundamental understanding of the physical mechanisms of bonding between ice and other solids.

This research project offered a new approach to solving the ice adhesion problem. Specifically, new experimental methods developed in Materials Science and Surface Physics, particularly the ability to examine ice/solid interfaces using molecular-scale microscopy, have been used. We applied several methods recently developed in scanning force microscopy and electrical spectroscopy of ice/solid interfaces to acquire information about the strength of molecular bonding between ice and various solids, thickness and viscosity of an interfacial liquid-like layer, and the spatial distribution of electric charges in the ice/solid interface.

We found that there are three major contributors to ice adhesion:

1) electrostatic interactions between the electrical charge at the ice surface and the charge induced on a solid substrate;

2) hydrogen bonding between water molecules and substrate atoms; and

3) Liftshitz-van der Waals (LVW) dispersion forces.

To eliminate or significantly reduce ice adhesion, all three types of interactions must be attacked.

The primary result of the study is a basic understanding of the nature of the strong and universal adhesion of ice to most solid materials. This understanding is based on the new knowledge of both the structure and physical properties of the ice-solid interface. The results have already permited purposeful development of a new type of active de-icing.

SUMMARY OF THE MOST IMPORTANT RESULTS

1. Effect of Electric Fields on Ice Adhesion

To determine the contribution of electrostatic interactions to ice adhesion, we measured the dependence of the work of adhesion or shear strength on three types of ice/metal interfaces.

1.1 Electrostatic Pressure: Doped Ice/Hg

The interface between ice and liquid mercury is convenient for measuring the work of adhesion W_A because in this case we are dealing with a solid/liquid interface and can apply the precise and powerful contact-angle technique to determine W_A :

$$W_A = \gamma_{Hg/Air}(1 + \cos\theta) \qquad (1)$$

where $\gamma_{Hg/Air}$ is the free energy of the Hg/air interface.

The electrostatic interactions between ice and a liquid metal may be very similar to those between ice and the same solid metal. Liquid mercury is also convenient in adhesion experiments because its surface can be easily cleaned and refreshed.

In the very first experiments, we indeed found that the application of a small DC bias caused dramatic changes in the adhesion of ice to mercury; see Figure 1. More precise measurements of the contact angle θ and the work of adhesion W_A were performed using a manometer made of ice with a thin channel filled with liquid mercury. When a potential difference was applied between the ice and mercury, the latter substance moved up or down depending on the change in W_A.

Figure 2 shows the effect of a DC bias on adhesion of ice doped with a small concentration of KOH. We studied this new effect on single-crystal ice and on polycrystalline ices, both pure and doped with NaCl, KOH, or HF. The temperature range was from –5°C to –20°C. We found that, depending on the bias polarity and magnitude, the work of adhesion can either be decreased by as much as 37-42% or increased by up to 70%. Electrostatic interactions of the electric charges in the interfacial double layer constitute the most plausible major mechanism of this phenomenon. The effect was not observed on very pure ice or under AC voltage, in which case high-density electric double layers did not form on the ice/metal interface.

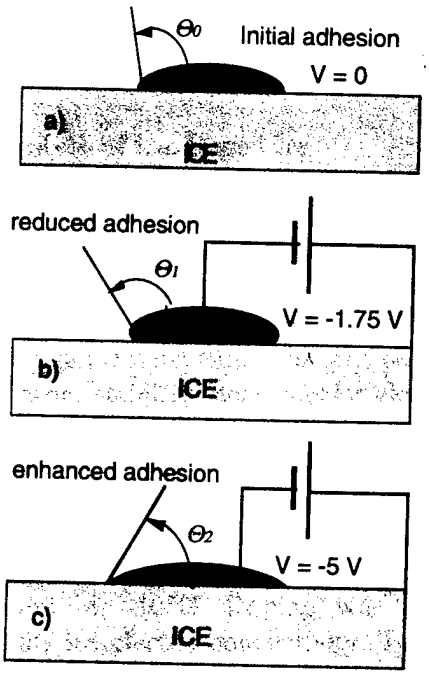

Figure 1. Schematic diagrams of the behavior of a mercury drop on the surface of ice grown from water doped with NaCl. T = –10°C.

Notice, that drastic changes in W_A were observed even when the voltage was below the threshold of ice electrolysis (±2V) and the electric current was very small. Hence, it was the effect of contact potential, not the effect of current.

Due to oxidation-reduction reactions, there is always some potential difference V_C, between a metal electrode and an electrolyte or such ionic conductor as ice [9]. Thus, the standard potential V_0 of mercury is +0.7958 V at 25°C. The real potential difference between a mercury electrode and a particular electrolyte depends on the electrolyte's pH, varying from about +0.9 V in very acidic solutions to about +0.2 V in very alkaline solutions.

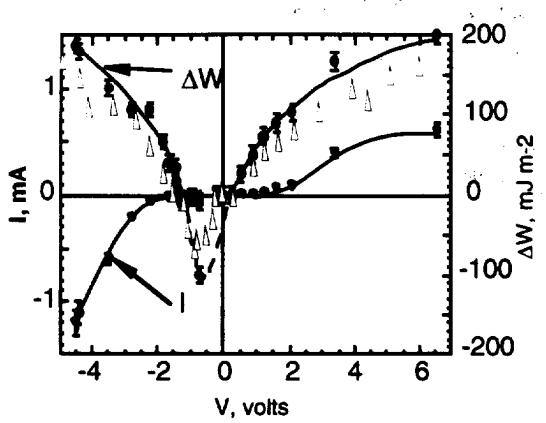

Figure 2. Graph showing the change in the work of adhesion ΔW and the current I (through a manometer type sample) versus DC bias V. Ice was grown from water doped with 0.2% KOH; $T = -10°C$. $W_A(0) = 293 \pm 25$ mJ/m^2.

The electric double-layer on the interface associated with this contact potential V_C consists of an atomically thin, positive charge of density $+\lambda$ on the mercury (or stainless steel) and an ionic space-charge $-\lambda$ in the subsurface layer of the electrolyte. The energy of the interfacial electric field is given by:

$$W'_{I/Hg} \approx \frac{\lambda \cdot V_C}{2} \approx \frac{C(V) \cdot V_C^2}{2} \qquad (2)$$

where $C(V)$ is an "apparent" interfacial capacitance that itself depends on V_C. The electrostatic portion of the work of adhesion is then given by:

$$W'_A = \frac{C(V) \cdot V_C^2}{2} \qquad (3)$$

When an external bias V is applied to the interface, W_A is given by:

$$W'_A = \frac{C(V) \cdot (V_C + V)^2}{2} \qquad (4)$$

which predicts a minimum W_A at $V = -V_C$. Such a minimum is seen in Figure 2. Substituting the experimentally found $C(V)$ and V_C predicts a magnitude of the minimum W_A of:

$$\Delta W_A = W'_A(0) - W'_A(V_C) \approx 160\ mJ/m^2$$

This is close to the value of 125±25 mJ/m^2 that was found experimentally.

Ryzhkin and Petrenko [3] performed a much more detailed and sophisticated calculation of the electrostatic energy of an ice/metal interface. They used a realistic spatial distribution of the electric field near the interface, which had been calculated earlier [4]. They have shown that, depending on the conditions at the interface, electrostatic forces can contribute up to 500 mJ/m^2 to the work of adhesion.

1.2 Electrolysis of Ice: Doped Ice

When liquid mercury was replaced as electrode material with stainless steel, the effect of electric current on ice adhesion dominated and masked the effect of electrostatic pressure [6-8]. Shear strength measurements were first performed on concentric, stainless steel, tubular electrodes. The shear apparatus that was used in these experiments is shown in Figure 3. The space between the inner and outer tubes was filled with a 0.5% solution of NaCl in water and the apparatus was then placed in a cold room with a temperature of −10°C. Doping was used to increase the ice electric conductivity. To reduce internal stress in the ice, all the samples were kept inside the cold room for 3 hours before they were tested. The maximum shear strength of the ice/steel interfaces was measured when the samples were loaded with a constant strain rate of 100 μm/min. A DC bias in the range 0–21 V was applied and maintained between the stainless steel tubes 1 minute prior to loading. A negative potential was always applied to the inner tube to prevent its electrocorrosion. It was found that the application of a small DC bias could indeed significantly reduce the interfacial strength, as seen in Figure 4. The interfacial current density in these experiments usually did not exceed 3 mA/cm^2.

To determine whether the application of DC power causes a change in ice temperature, a thin thermocouple was placed in the ice between the steel tubes in several tests. Within the precision of those tests (±0.05°C), we did not find any temperature change when the voltage was ≤15 V. When a bias of 21 V was applied to the interface, we observed a 0.5°C temperature rise. This cannot account for the almost 10-fold drop in the

interface strength because, in the control experiments, heating the apparatus by 1°C (to −9°C) caused only a 10% change in the shear strength of the interface. Moreover, application of 20 V of 60Hz AC voltage, that generated the same heat, didn't produce any measurable change in the interfacial strength. Direct optical examination of the interfaces under direct current showed intensive generation of gas bubbles (H_2 and O_2) released during ice electrolysis. The bubbles reduce the contact area between the ice and electrodes and initiate interfacial cracking, thus weakening the interfaces.

1.3 Electrolysis of Ice: Pure Ice

Because pure ice has very low electric conductivity, we reduced the inter-electrode spacing to 50 μm to provide sufficient density of the current (1 to 10 mA/cm^2). For making circuits of that scale we used photolithography. The interdigitated electrodes were made of 5-μm-thick copper foil electroplated with gold. Copper-clad laminate on 125-μm kapton film was used for this purpose. We first formed copper grids using photolithography, followed by chemical etching. The electrodes were then electroplated with gold to enhance their resistance to electrocorrosion; see Figure 5. Figure 6 shows a schematic of the electric circuit used to apply DC voltage to the grids covered with ice and/or water. We used pure distilled water with conductivity of 2 to 5 μS in these experiments.

Prior to freezing the water, a small DC bias of 4 to 5 V was applied to the electrodes to form a double layer of electric charges on the electrodes. After the water was frozen, the double layers provided good charge exchange between the ice and metal electrodes (so-called "ohmic electrodes") [10].

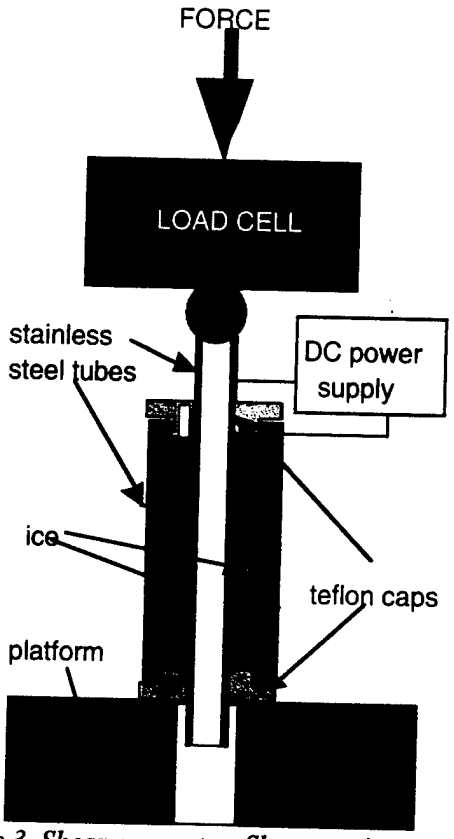

Figure 3. Shear apparatus. Shear strain occurs on the interface between the inner stainless steel tube and ice. T = −10°C.

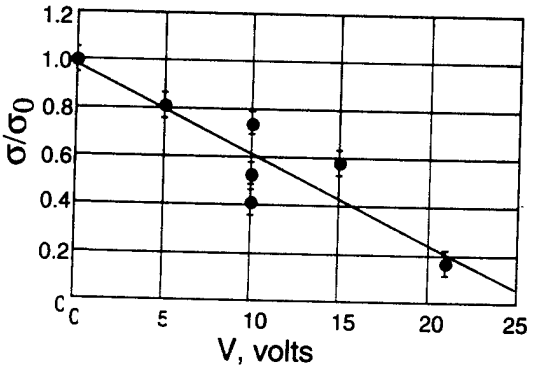

Figure 4. The relative shear strength of the ice/steel interface, σ/σ_0, versus the voltage applied between the inner and outer steel tubes. T = −10°C, strain rate = 100 μm/s. The water was doped with 0.5% NaCl.

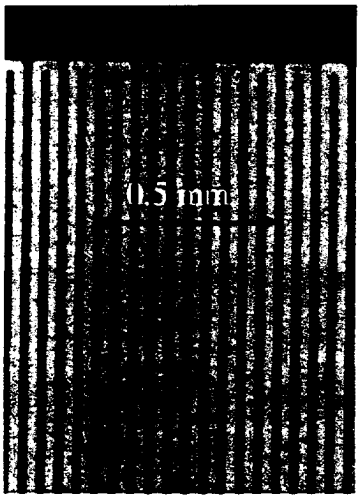

Figure 5. Copper-grid electrodes electroplated with gold on 125-μm kapton film. The electrodes appear dark in transmitting light

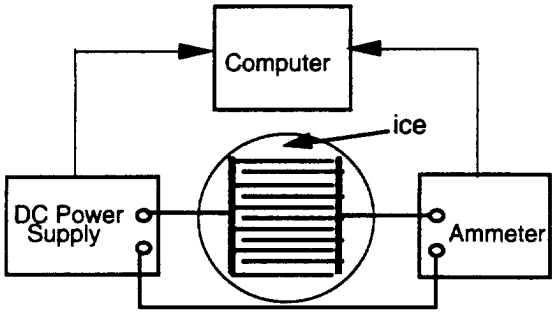

Figure 6. Electric circuit used in this study.

A graph of current density versus voltage dependence of the grid/ice system, shown in Figure 7, demonstrates a rapid rise in current density when the voltage exceeds the ice-electrolysis threshold, 2 V. We noticed that it takes a higher voltage, ≥5V, to produce gas bubbles, as seen in Figure 8.

The electric current passing through the ice/metal interface generates electrolytic gases, H_2 and O_2 [11], thus doing irreversible damage to the interface. The initial stage of this gas generation can be seen in Figure 8. Under high-voltage currents the interface can ultimately be destroyed, with subsequent decay of the current to zero.

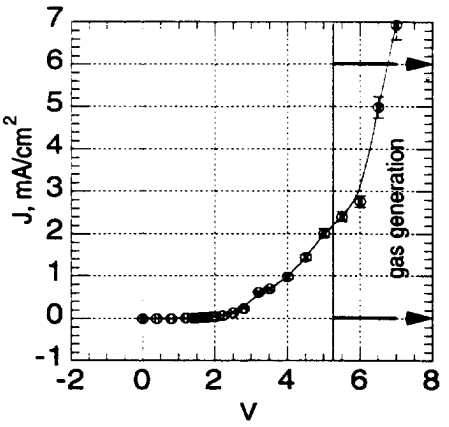

Figure 7. Current-voltage characteristics of a gold grid covered with pure ice. T = –10°C.

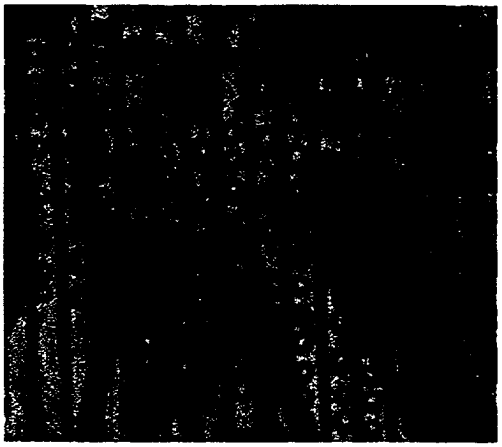

Figure 8. Initial stage of bubble generation on a gold grid in ice as seen 10 s after 6 volts was applied. T = –10°C. The small circular bubbles were generated on the interface by ice electrolysis. The large gas bubbles of odd shapes were formed in the ice bulk during freezing.

The effect of electric currents on the strength of ice/grid interfaces was studied using the shearing apparatus shown in Figure 9. Ice/grid interfaces were tested in the temperature range from –5°C to –25°C. Pure distilled water was placed between the shearing metal plates, as shown in Figure 9. Then a DC bias of 5 V was applied to the grid and the water was frozen.

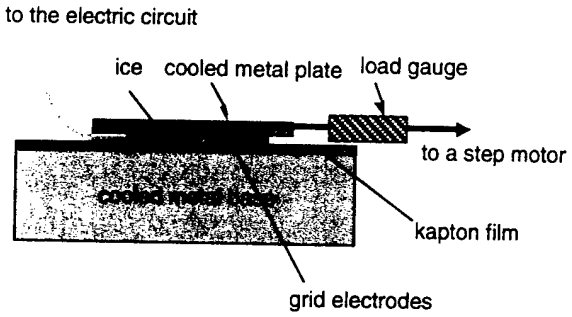

Figure 9. Mechanical apparatus for shear-strength tests.

The voltage was then increased to provide passage of the total charge Q (up to 5 C/cm^2) during 1 minute. After that the interface was loaded to the breaking point and the maximum shear force was recorded. A strong effect of the DC bias on ice adhesion strength was found in these tests, as illustrated in Figure 10.

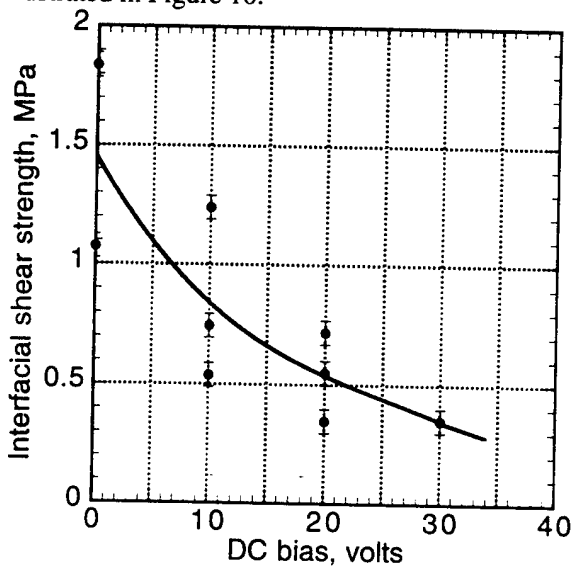

Figure 10. Dependence of shear strength of the ice/grid interface on voltage applied after the ice was formed. Pre-applied voltage was 5 V. T = -8°C.

In most of the 5 C/cm^2 tests, the ice/grid interfaces were completely destroyed by the current. Notice that the residual interfacial strength was well below those known for the best solid anti-icing coatings.

Our results demonstrated the importance of pre-applied voltage that forms electric double layers on ice/metal interfaces. Without these layers the current was small and the de-icing effect was almost absent.

2. Scanning Force Microscopy

(Nickolayev and Petrenko, 1995; Petrenko, 1997)

Scanning force microscopy is specifi-cally suitable for the study of ice adhesion, since various modes of SFM combine near atomic–scale spatial resolution with the ability to test a wide variety of physical parameters, such as density of surface charge, QLL viscosity, micro-hardness, liquid film thickness, adhesion strength, etc. (see, for example, Binning, 1992; Sarid, 1991; Burnham and Colton, 1991; Hoh et al., 1992; and Weisenhorn et al., 1992). Nevertheless, in applying SFM to ice a researcher faces some challenging experimental problems. The first is the effect of a hot cantilever tip on the ice surface being investigated. Due to the electrical power dissipated on a piezolever or the heat of a laser beam, the tip temperature under typical experimental conditions can exceed the ambient temperature by 10°C (Eastman and Zhu, 1995). This forces the researcher to decrease the DC bias applied across the piezolever or decrease the laser beam intensity, at the cost of a reduced signal-to-noise ratio.

The second experimental difficulty is the strong and time-dependent adhesion of ice to tips, which often ultimately results in tip capture and breakage. In the pioneering SFM experiments on ice, these problems were successfully overcome and encouraging preliminary experimental results were obtained (Nickolayev and Petrenko, 1995; Slaughterbeck et al., 1996; Petrenko, 1997). Brief descriptions of the technique and the principal results are given below.

2.1 Experimental Technique

Scanning force microscopy experiments on ice must provide very good temperature and humidity control. Otherwise, surface evaporation or sublimation may produce rapid changes in the ice surface topography. A large temperature gradient may also cause intensive mass transport in the QLL, contributing to instability of SFM images.

We used an AutoProbe SA microscope with a 100-μm scanner (Park Scientific Instruments, Sunnyvale, California). The microscope can operate in both contact and non-contact modes. Both high-voltage and low-voltage regimes of the scanner were employed, depending on the needed ranges of lateral and vertical scanning.

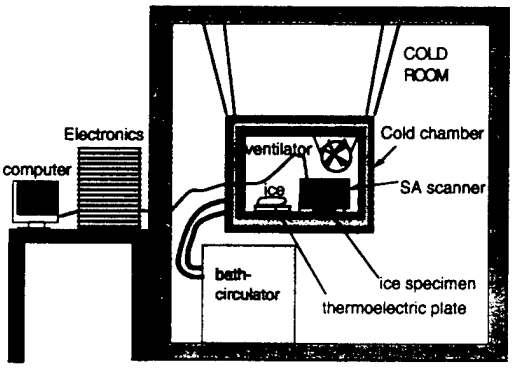

Figure 11. Experimental arrangement used in scanning force microscopy of the surface of ice.

To decrease the power released on a piezolever, the scanner electronics were modified; namely, we decreased the DC bias applied to the piezolever from 1.25 V to 0.116 V. This made the electrical power scattered on the cantilever equal to 6.7 μwatt. An estimate similar to one made by Eastman and Zhu (1995) showed that in our experiments the temperature at the tip of the piezolever differed by less than 0.1°C from the ambient temperature when measurements were performed in air and by less than 0.01°C when the piezolever was immersed in decane.

To compensate for the decrease in sensitivity, we modified the scanner pre-amplifier, making its gain factor equal to 1000 instead of 100. In addition, we shielded all the cables which connect the scanning head with the controlling electronics. The modified preamplifier significantly improved the signal-to-noise ratio.

We have used Si and Si_3N_4 (silicon nitride) piezolevers with spring constants of 2.5 N/m and 20 N/m. The softer cantilevers were used in the contact mode experiments, while the stiffer ones were used in the non-contact tests. The radius of the tip curvature, R, was measured using a Nb tip-calibration artifact (General Microdevices Inc., Edmon-ton, AB, Canada). The value of R ranged from 30 nm to 120 nm for different tips.

We calibrated the z-, x-, and y-detectors of the scanner once a week at each particular temperature used in the study. The possibility of pressure melting of the ice surface under the action of a tip has been discussed by Nickolayev and Petrenko (1995) and by Petrenko (1997). It should be noted here that at $T \leq -1.5$°C such melting has never occurred in our SFM tests, due to plastic relaxation of contact stress in ice (Barns et al., 1971).

The scanner was enclosed in a sealed environmental chamber in which temperature and humidity were kept constant during the experiments; see Figure 11. The temperature was maintained in the range from 0°C to –20°C with ± 0.05°C precision, and relative humidity was maintained in the range from 25% to 97% with ± 1% precision.

The environmental chamber had internal dimensions of 25 cm × 25 cm × 25 cm. A tiny "computer-chip" ventilator hung on four thin rubber strips and stirred air inside the chamber. The chamber was installed on a massive (60 kg) concrete platform and the latter hung from eight "tie-on," 4-foot long rubber strips, to minimize vibration from within the building generated by refrigeration system motors in the Ice Research Laboratory. The frame supporting the concrete platform and the environmental chamber on it were placed inside a large cold room in which we maintained the same temperature as in the chamber but with less precision (± 0.5°C). Work in the cold room permitted us to prepare, load, and change ice samples without exposing them to thermo-shock and without deposition of frost micro-crystals onto the smooth ice surface. The microscope controller and computer were kept outside the cold room.

We used single crystals of pure ice grown using the fast growth technique. The (0001) face of the crystals was smoothed by a microtome machine and gently polished with an optically smooth quartz plane. The ice specimens had dimensions of 10 mm × 10 mm × 1 mm, with the basal plane as their wider face. The samples were frozen at the bottom to a thick aluminum plate whose temperature was well controlled. When conductive Si cantilever tips were used, the potential difference between the tips and the

electrically grounded ice samples was only 57 mV, with the "plus" on the cantilever tips.

In some experiments a drop of pure liquid decane (for analysis) was placed on the top of an ice sample, providing a 0.5- to 1.0-mm thick liquid film. Decane was chosen for its insolubility in water and its low freezing point, low vapor pressure, and low viscosity. In these experiments the piezolever and the ice surface were completely covered with decane.

2.2 SFM Results

Prior experimental results obtained with the SFM technique on the ice surface were described in detail in our recent publications (Nickolayev and Petrenko, 1995; Petrenko, 1997). Some of the essential experimental facts which explain the potential power of this technique in application to ice are discussed below.

First, the SFM proved to be very useful in studying the QLL on the ice surface and on ice/liquid and ice/solid interfaces. The SFM can detect the presence of a QLL, measure its thickness, and with the aid of theoretical calculations can determine the viscosity of the QLL.

When a QLL appears on the ice surface, it smoothes and flattens the surface due to intensive mass transport in the surface layer. For example, a well created during intensive scanning of a small area of ice surface (see Figure 5) remains on the surface for about one hour at T = –20°C but "heals" in a few seconds at –10°C, when the QLL can be detected. Theoretical calculations showed that the healing time τ_H depends on the QLL thickness d and viscosity ν, as follows:

$$\tau_H = 2\nu\gamma a^4 d^{-3} \qquad (5)$$

where γ is the interfacial tension (of ice/ liquid or ice/air interfaces) and d is the QLL thickness. Thus, if any two parameters of γ, ν, and d are known, measurements of τ_H will provide the third one.

Figure 12. A well formed on the ice surface during the scanning procedure. Ice surface under decane, T = –20.0°C, set point = 50 nN, scanning frequency = 1 Hz, Si_3N_4 tip. The well depth is 0.22 μm, its width is 7.5 μm, and the banks' height = 0.23 μm.

Second, so-called force curves (FC) can be used to determine: 1) the QLL thickness on ice/air, ice/metal, and ice/liquid interfaces; 2) the density of surface or interfacial charges; and 3) the work of ice adhesion to the tip material and different coatings. In the FC mode a cantilever tip moves up and down while the tip-sample force and tip-sample distance are recorded. In this method, the amount of force and the spatial resolution are mainly limited by ambient acoustic vibration. In our case they were respectively 1 nN, which is about the strength of one hydrogen bond, and 0.3 nm. From a force curve a wealth of information about the properties of the surface can be extracted. For instance, one can determine the type of tip-surface interaction, the adhesion "pull-off" force, and the thickness of a liquid film present on the surface (Burnham et al., 1991; Hues et al., 1993; Weisenhorn et al., 1992).

Figure 13 shows schematically the "anatomy" of a force curve derived from an ice surface in air. The sudden dip of the cantilever tip on approach is due to a capillary force exerted on the tip by the QLL. The thickness of the QLL determined by this method on the (0001) face of very pure ice was 3.45 ± 0.4 nm at –10°C and coincided well

with the most reliable data obtained by glancing angle x-ray scattering (Dosch et al., 1996).

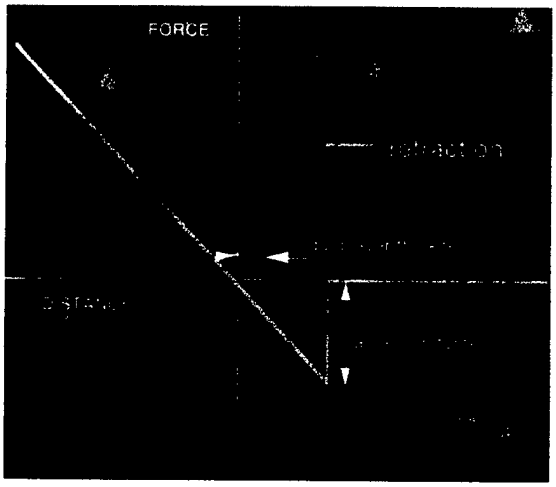

Figure 13. Anatomy of a force curve.

The pull-off (adhesion) force shown schematically in Figure 6 can be used to cal-culate the ice/tip-material interfacial energy. This force is simply proportional to the interfacial energy:

$$F = -4 \pi R \gamma_{sv} \qquad (6)$$

where γ_{sv} is the ice/Si_3N_4 interfacial energy in the presence of water vapor (Israelashvily, 1991). Substitution of the typical pull-off force observed at T = –10°C, F = (100 ± 15) nN, gives $\gamma_{sv} \approx$ (80 ± 12) mJ/m^2.

We found that SFM of the ice surface in decane has several advantages. First, a layer of decane prevents ice evaporation, thus making the ice surface much more stable. Second, the capillary forces between the QLL and a cantilever tip become very small and do not affect the microscope operations. In fact, in our experiments with cantilevers immersed in decane, the capillary forces were so small that we could not distinguish them from the electrical noise. Third, in decane the adhesion force applied to Si_3N_4 tips was absent or small. In the absence of the capillary and pull-off forces a significant remote repulsion between the tip and ice surface becomes apparent. This repulsion appeared only after several contacts between the tip and the surface and was interpreted as an electrostatic repulsion between two like charges sitting on the tip and on the ice surface. Most probably the tip acquires the charge from the ice surface. Assuming that both surface charges have the same density, λ_S, one can easily calculate that density when the tip geometry is known. In the temperature range from –0.5°C to –20°C, $\lambda_S \approx 10^{-2}$C/m^2 and within the data scattering λ_S did not seem to depend on temperature; see Figure 14.

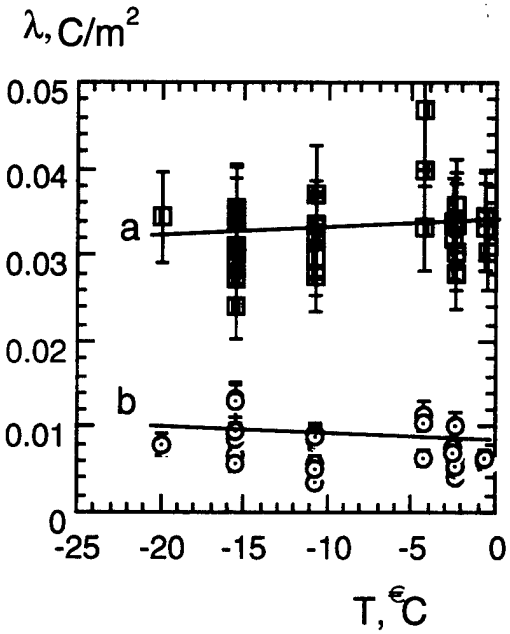

Figure 14. The surface charge density λversus temperature, calculated in approxi-mation of elastic (a) and plastic (b) inter-action between a tip and the ice surface.

The value of $\lambda_S \approx 10^{-2}$C/m^2 is of the same order of magnitude as that calculated by Kroes (1992), and also is similar to that found as an upper limit of the surface charge density estimated using frictional electrifi-cation of ice (Petrenko and Colbeck, 1995).

Finally, we succeeded in obtaining SFM images of ice/metal interfaces; see Figure 8. In these experiments pure water was frozen in contact with a vertical indium wall. Then a sharp microtome blade was used to cut the top of the ice/metal interface. The blade moved parallel to the interface to prevent production of burrs. Images of such an interface acquired in contact, taping, and non-contact modes revealed a

transition layer that we believe is a quasi-liquid layer between ice and indium.

Similar images can also be acquired when the interface is immersed in decane, thus preventing ice evaporation. This technique provides an easy and convenient method to study an interfacial QLL from the side; for example, the layer thickness and viscosity can be determined. Any soft and cuttable material, such as a plastic, can be used to prepare an interface which is smooth enough for SFM.

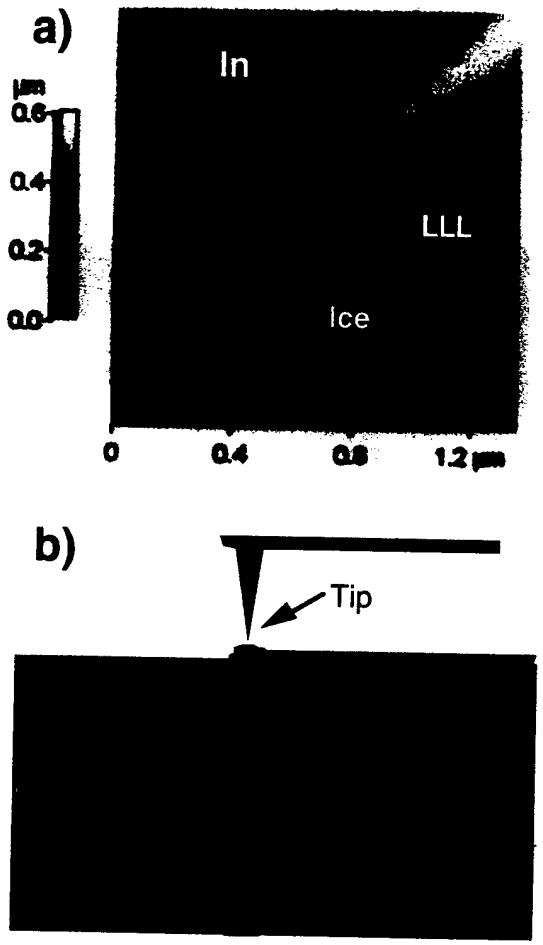

Figure 15. SFM image of an ice/In interface (a) and its interpretation (b). The image was acquired in air at _1‰ÚC_using contact mode.

3. Electrical Spectroscopy

(Khusnatdinov, Petrenko and Levey 1997)

We used a field effect transistor made of ice to determine the surface charge charac-teristics of ice/insulator and ice/metal inter-faces. When the subsurface space charge consists mainly of one type of charge carrier (majority charge carrier), then the layer's total charge λ_s and its thickness L can be determined by measurements of the contact electric potential V_c, surface conductivity σ_s, and surface capacitance C_{int}:

$$V_c \approx (\lambda_s L)/(\varepsilon_0 e) \quad (7)$$

$$\sigma_s \approx \mu \cdot |\lambda_s| \quad (8)$$

$$C_{int} \approx (\varepsilon_0 e)/L \quad (9)$$

where μ is the charge carrier mobility. V_c and C_{int} of an ice/**metal** interface can be determined from AC data on conductivity and capacitance of the interface measured as functions of an externally applied DC bias, V_b. When $V_b = -V_c$, the capacitance of the interface passes a minimum. To find V_c and C_{int} of an ice/**insulator** interface, we used and will use a field effect transistor (FET) made of ice that was first invented by Petrenko and Maeno in 1987 and further improved recently by Khusnatdinov et al. (1997); see Figure 16.

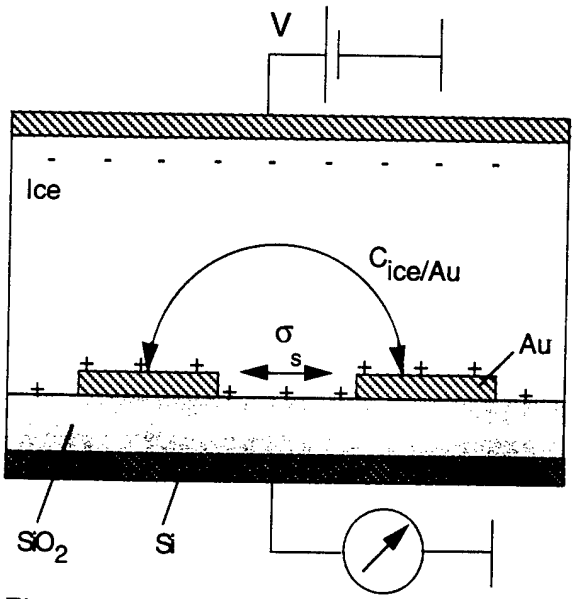

Figure 16. Schematics of an ice field effect transistor. Inter-electrode spacing and the electrode width were 50 μm.

In this method the conductivity of ice/SiO_2 and the capacitance of ice/SiO_2 and ice/gold interfaces are measured in a wide frequency range while a DC bias is applied across the ice/SiO_2

interface. It was found that the surface conductivity and surface charge depend nonlinearly on the bias applied to the surface as the bias changes within the limits of ±1 V. Application of the bias irreversibly changed the conductivity and surface charge of the ice. Depending on the preparation procedure, annealing time, and bias history, the surface charge can be negative or positive within the limits of $\pm 1 \times 10^{-4}$ C/m^2 and can be easily modified by an external DC bias.

4. Effect of self-assembling monolayers on ice adhesion to metals

Strong adhesion of ice to almost all known solids is a serious engineering problem that has not been solved yet because physical mechanisms of ice adhesion are not understood. In this research we used an original method to study the role of hydrogen bonding in ice adhesion and to minimize the effect of this mechanism on ice adhesion. For this purpose, we coated metals (Au and Pt) with a mono-molecular layers of specific organic molecules that had either strong hydrophobic properties (CH3(CH2)11SH) or strong hydrophilic properties (OH3(CH2)11SH), see figure 17. To determine the contribution of hydrogen bonding to ice adhesion SAMs of varying hydrophobia/hydrophilia were made by mixing the hydrophobic and hydrophilic components. All the films were built of similar molecules that differed only in their outermost groups, OH- and CH3. Thus, when the films were grown on the same substrate (almost atomically smooth metal films) any difference in their adhesion to ice were due to the difference in the hydrogen bonding between the ice and SAM's. The films' structure and quality were examined with SPM and the degree of SAM's hydrophobia/hydrophilia was characterize with a contact angle of water on the films. We have then frozen water on the films and measured shear strength of ice/SAM/metal interfaces. Possible damage to the interfaces was examined with SPM after the ice was melted. We found a strong correlation between the degree of hydrogen bonding and the ice adhesion strength, figure 18. Though, the hydrogen bonding was found neither single nor major mechanism contributing in ice adhesion.

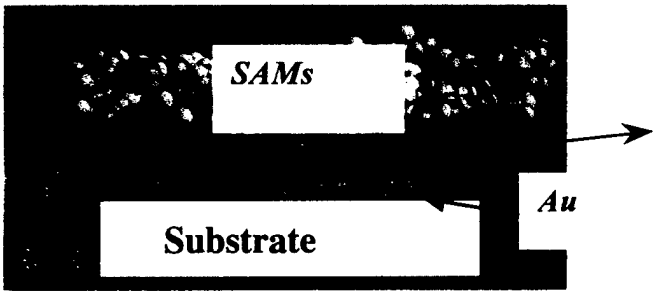

Figure 17. A schematic diagram showing the structure of SAMs bound to the gold surface.

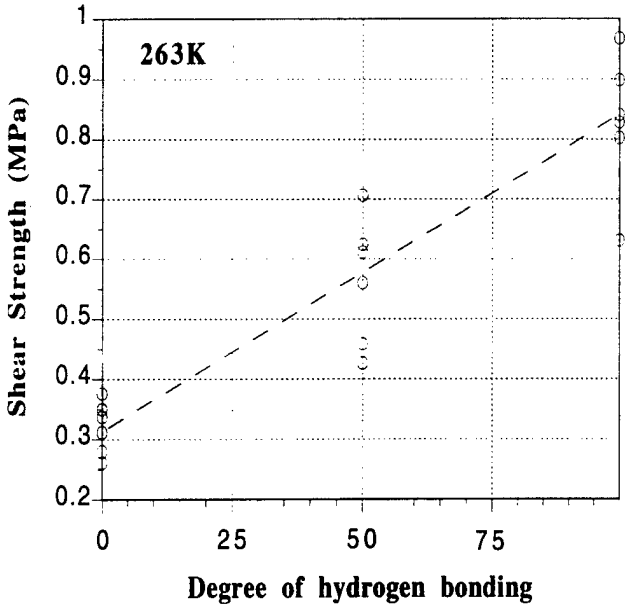

Figure 18. Effect of degree of hydrogen bonding on the ice/SAM shear strength.

5. List of Publications

Journal Publications:

1. Khusnatdinov N. N. and Petrenko V. F. (1996) Fast-growth technique for ice single crystals. *J. Crystal Growth.*, **163**:420-425.
2. N. N. Khusnatdinov and V. F. Petrenko: Experimental study of ice electrolysis in darkness and under ultraviolet irradiation. Journal of Physical Chemistry, vol. 101, 6208-6211 (1997).
3. N. N. Khusnatdinov, V. F. Petrenko, and C. Levey: Electric properties of ice/solid interface. Journal of Physical Chemistry, vol. 101, 6212-6214 (1997).
4. V. F. Petrenko: Study of ice surface and ice/solid interfaces with scanning force microscopy. Journal of Physical Chemistry, vol. 101, 6276-6281 (1997).
5. I. A. Ryzhkin and V. F. Petrenko: Physical mechanisms responsible for ice adhesion. Journal of Physical Chemistry, vol. 101, 6267-6270 (1997).
6.V. F. Petrenko and I. A. Ryzhkin: Surface states of charge carriers and electric properties of the surface layer of ice. Journal of Physical Chemistry, vol. 101, 6285-6289 (1997).
7.V. F. Petrenko: Effect of electric fields on ice adhesion to mercury. Journal of Applied Physics, vol. 84, 261-267 (1998).
8.V. F. Petrenko and S. Qi: Effect of electric field on ice adhesion to stainless steel. Journal of Applied Physics, vol. 86, 5450-5454 (1999).

Other Publications:

9.V. F. Petrenko: Methods and apparatus for modifying ice adhesion strength. World Intellectual Property Organization. PCT. International Publication Number WO 98/57851, 23 December 1998.

Book:

10. V. F. Petrenko and R. W. Whitworth: Physics of Ice. Oxford University Press (1999).

6. Sientific of participating scientificpersonnel

1. Victor F. Petrenko, PI, Research Professor of Engineering.
2. Niyaz Khusnatdinov, PhD student, post doctoral research associate.
3. Douglas Trickett, PhD student
4. Zoe Courville, PhD student
5. Rafael Hernandez, undergraduate (work-study) student
6. Frank Black, undergraduate student

7. Report of Inventions

1. Systems and Method for modifying Ice Adhesion Strength. United States Patent #6,027,075, Feb 22, 20000.
2. USP Provisional Application, Attorney docket No. 4503/009P, filed October 27, 1998.
3. USP Provisional Application, Attorney docket No. 4503/009P2, filed December 1, 1998.
4. USP Provisional Application, Attorney docket No. 4503/009P3, filed March 1, 1999.
5. USP Provisional Application, Attorney docket No. 4503/009P4, filed April 23, 1999.
6. World Intellectual Property Organization (WIPO) patent application, WO9857851A2, filed December 23, 1998.

Bibliography

Allara, D. L. and Nuzzo, R. G. (1985) *Langmuir, 1*: 45-52.

Bascom, W. D., Cattington, R. L. and Singleterry, C. R. (1969) Ice adhesion to hydrophilic and hydrophobic surfaces. *J. Adhesion,* 1: 246-263.

Binning, G. (1992) Force Microscopy. *Ultramicroscopy, 42-44*: 7-15.

Burnham, N. A. and Colton, R. J. (1991) Interpretation issues in force microscopy. *J. Vac. Sci. Technol. A,* 9(4): 2548-56.

Churaev, N. V., Bardasov, S. A. and Sobolev, V. D. (1993) On the non-freezing water interlayers between ice and a silica surface. *Colloids and Surfaces A: Physicochemical and Engineering Aspects,* 79: 11-24.

Croutch, V. K. and Hartley, R. A. (1992) *J. Coatings Technology. 64* (815), 41.

Dosch, H, Lied, A. and Bilgram, J. H. (1996) Disruption of the hydrogen-bonding network at the surface of ice Ih ice near surface premelting . *Surface Science 366*: 43-50.

Dzyaloshinskii, I.E., Lifshitz, E.M. and Pitaevskii, L.P. (1961) The General Theory of Van-der-Waals Forces. *Advances in Physics*, 10: 165-209.

Eastman, T. and Da-Ming Zhu (1995) Influence of an AFM tip on interfacial melting on ice. *J. Coll. Interface Sci. 172*: 297-301.

Hays, D.A. In *Fundamentals of Adhesion,* Ed. Lee, L.H.; Plenum Press: New York, 1991; Chapter 8.

Hickman, J. J., Zou, C., Ofer, D., Harvey, P. D., Wrighton, M. S., Laibinis, P. E., Bain, S. D. and Whitesides, G. M. (1989) *J. Am. Chem. Soc., 111*: 7271-72.

Hoh, J. H., Cleveland, J. P., Prater, C. B., Revel, J. P. and Hansma, P.H. (1992) Quantized adhesion detected with the Atomic Force Microscope. *J. Amer. Chem. Soc.* 114: 4917-18.

Israelashvili, J. (1991) *Intermolecular and surface forces,* Academic Press: London, Chapter 15.

Itagaki, K. (1983a) The implication of surface energy in ice adhesion. *J. Adhesion,* 16: 41-48.

Jellinek, H.H.G. (1959) Adhesive Properties of Ice. *Journal of Colloid Science,* 14: 268-79.

Jellinek, H.H.G. (1962) Ice Adhesion. *Canadian Journal of Physics,* 40: 1294-309.

Jellinek, H.H.G. (1967) Liquid-like (Transition) Layer on Ice. *Journal of Colloid and Interface Science,* 25: 192-205.

Khusnatdinov, N. N.; Petrenko, V. F. (1996)*J. Crystal Growth, 163*: 420-25.

Khusnatdinov, N. N.; Petrenko, V. F. and C. Levey (1997) " Electrical Properties of Ice/Solid Interface", *J. Phys. Chem. , 101(32):* 6212-14.

Kroes, G. J. (1992) Surface melting of the (0001) face op TIP4P ice. *Surface Science* 275: 365-82.

Landy, M. and Freiberger, A. (1967) Studies of Ice Adhesion. I. Adhesion of Ice to Plastics. *Journal of Colloid and Interface Science, 25*: 231-44.

Lee, H., Kepley, L. J., Hong, H., Akhter, S.and Mallouk, T. E. (1988) *J. Phys. Chem., 92*: 2597-2601.

Maoz, S. and Sagiv, J. (1987) *Langmuir, 3*: 1045-51.

Nickolayev, O. and Petrenko, V. F. (1995) SFM studies of the surface morphology of ice, *MRS Symposium Proceedings, edited by B. G. Demczyk et al., 355*: 221-26, MRS, Pittsburgh.

Nuzzo, R. G., Allara, D. L. *J. Am. Chem. Soc.* (1983) *105*: 4481-83.

Petrenko, V. F. (1997a) Study of ice surface, ice/solid and ice/liquid interfaces with SPM. *J. Phys. Chem. **101**(32)*:6276-81.

Petrenko, V. F. (1997b) " Method and apparatus for modifying ice adhesion strength", *U.S. Provisional Patent Application Serial No.: 60/049,790 June 16, 1997*).

Petrenko, V. F. and E. M. Schulson (1993) Action of electric fields on plastic deformation of pure and doped ice single crystals, *Phil. Mag.* A, 67: 173-85.

Petrenko, V. F. and Ryzhkin, I. A. (1997) "Surface states of charge carriers and electrical properties of the surface layer of ice", *J. Physical Chemistry, 101(32):* 6285-89.

Petrenko, V.F and Maeno, N. (1987) Ice Field Transistor. *Journal de Physique C1,* 48: 115-9.

Petrenko, V.F. and Colbeck, S.C. (1995) Generation of Electric Fields in Ice and Snow Friction. *J. Appl. Phys.,*: *77(9)*:4518-21.

Pittenger, B., Cook, D. J., Slaughterbeck, C. R. and S. C. Fain, Jr. (1998) "Investigation of ice-solid interfaces by force microscopy: plastic flow and adhesive force."*J. of Vacuum Science &Technology A 16,1832-7.*

Porter M. D.., Bright, T. B., Allara, D. L. and Chidsey, C. E. D. (1987) *Langmuir,* 5:3559-68.

Raraty, L.E. and Tabor, D. (1958) The Adhesion and Strength Properties of Ice. *London: Proceedings of Royal Society,* A245: 184-201.

Reubinstein, I., Steinberg, S., Tor, Y., Shanzer, A. and Sagiv, J. (1988) *Nature,332*:426-29.

Ryzhkin, I. A. and Petrenko, V. F. (1997) Physical mechanisms responsible for ice adhesion. *J. Phys. Chem. , **101**(32):* 6267-70.

Ryzhkin, I.A. (1985) Superionic Transition in Ice. *Solid State Communications*, 56: 57-60.

Sarid, D. (1991) *Scanning Force Microscopy*, New York: Oxford Univesity Press.

Slaughterbeck, C. R.; Kukes, E. W.; Pittenger, B.; Cook, D. J.; Williams, P. C.; Eden, V. L.; Fain, S. C. (1996) *J. Vac. Sci. Technol. A, 14(3)*: 1213.

Stoneham, A.M.; Tasker, P.W. *J. Phys. C: Solid State Physics.* (1985) *18*, L543.

Takahashi, T. (1969a) Electric Potential of Liquid Water on an Ice Surface. *Journal of Atmospheric Science,* 26: 1253-8.

Takahashi, T. (1969b) Electric Potential of Rubbed Ice Surface. *Journal of Atmospheric Science,* 26: 1259-65.

Tillman, N., Ulman, A. and Elman, J. F. (1989) *Langmuir, 5*: 1020-26.

Van Oss, C. J., Giese, R. F., Wentzek, R., Norris, J. and E. M. Chuvilin (1992*) J. Adhesion Science and Technology. 6(4*: 503.

Weisenhorn, A. L., Maivald, P., Butt, H.-J. and Hansma, P. K. (1992) Measuring of adhesion, attraction and repulsion between surfaces in liquids with an atomic-force microscope. *Phys. Rev. B.* 45(19): 11226-232.

Whitesides, G. M. *Chimia* (1990) *44*: 310-11.

Wilen, L. A., Wettlaufer, J. S., Elbaum, M. and M. Schick (1995) Phys. Rev. B., *52(16):* 12426.